

Paired Ru–O–Mo ensemble for efficient and stable alkaline hydrogen evolution reaction

HuangJingWei Li,^{a,b†} Kang Liu,^{a†} Junwei Fu,^{a,*} Kejun Chen,^a Kexin Yang,^a Yiyang Lin,^a Baopeng Yang,^a Qiyu Wang,^a Hao Pan,^c Zhoujun Cai,^a Hongmei Li,^a Maoqi Cao,^{a,e} Junhua Hu,^d Ying-Rui Lu,^f Ting-Shan Chan,^f Emiliano Cortés,^g Andrea Fratalocchi,^b and Min Liu^{a,*}

^aState Key Laboratory of Powder Metallurgy, Hunan Provincial Key Laboratory of Chemical Power Sources, School of Physics and Electronics, Shenzhen Institute of Central South University, Central South University, Changsha 410083, P. R. China.

Email: fujunwei@csu.edu.cn, minliu@csu.edu.cn

^bPRIMALIGHT, Faculty of Electrical and Computer Engineering, King Abdullah University of Science and Technology (KAUST), Thuwal, 23955-6900, Saudi Arabia.

^cDepartment of Periodontics & Oral Mucosal Section, Xiangya Stomatological Hospital, Central South University, 72 Xiangya Road, Changsha, Hunan, PR China.

^dSchool of Materials Science and Engineering, Zhengzhou University, Zhengzhou, 450002, P. R. China.

^eSchool of Chemistry and Chemical Engineering, Qiannan Normal University for Nationalities, Duyun 558000, P. R. China.

^fNational Synchrotron Radiation Research Center, Hsinchu 300, Taiwan.

^gChair in Hybrid Nanosystems, Nano-Institute Munich, Faculty of Physics, Ludwig-Maximilians-Universität München, München 80539, Germany.

† These authors contributed equally.

Abstract

Electrocatalytic hydrogen evolution reaction (HER) in alkaline media is a promising electrochemical energy conversion strategy. Ruthenium (Ru) is an efficient catalyst with a desirable cost for HER, however, the sluggish H₂O dissociation process, due to the low H₂O adsorption on its surface, currently hampers the performances of this catalyst in alkaline HER. Herein, we demonstrate that the H₂O adsorption improves significantly by the construction of Ru–O–Mo sites. We prepared Ru/MoO₂ catalysts with Ru–O–Mo sites through a facile thermal treatment process and assessed the creation of Ru–O–Mo interfaces by transmission electron microscope (TEM) and extended X-ray absorption fine structure (EXAFS). By using Fourier-transform infrared spectroscopy (FTIR) and H₂O adsorption tests, we proved Ru–O–Mo sites have tenfold stronger H₂O adsorption ability than that of Ru catalyst. The catalysts with Ru–O–Mo sites exhibited a state-of-the-art overpotential of 16 mV at 10 mA cm⁻² in 1 M KOH electrolyte, demonstrating a threefold reduction than the previous bests of Ru (59 mV) and commercial Pt (31 mV) catalysts. We proved the stability of these performances over 40 hours without decline. These results could open a new path for designing efficient and stable catalysts.

Keywords: alkaline HER, H₂O adsorption, MoO₂, Ru, Ru–O–Mo sites

1. Introduction

The production of hydrogen from H₂O is considered one of the most promising approaches to meet the present and future demand for renewable electricity storage.[1-4] Currently, industrial hydrogen is mostly produced by electrolyzing H₂O in alkaline solutions, involving hydrogen evolution reaction (HER) on cathodes and oxygen evolution reaction (OER) on anodes. One of the main issues that hamper the development of efficient systems lies in the slow HER kinetics in alkaline solutions, requiring the engineering of catalysts with sufficiently low overpotentials to drive the hydrogen reaction.[5-8]

In alkaline solutions, a fast HER kinetics requires the rapid dissociation of H₂O and the subsequent hydrogen desorption.[9-13] Recently, ruthenium (Ru) has attracted attention as an ideal HER candidate with hydrogen (H*) adsorption energy (65 Kcal mol⁻¹) similar to the state-of-the-art Pt (62 Kcal mol⁻¹),[14-16] at a cost that is 25 times smaller than the cost of Pt.[17-19] However, the weak H₂O adsorption and dissociation ability of Ru is a significant obstacle for fully exploiting the high intrinsic activity of this material in alkaline HER. The main issue is the weak interaction between the 4d orbitals of Ru and the 2p orbitals of the oxygen in H₂O molecules.[20,21] The construction of properly paired M1–O–M2 (M means Metal) sites could be a promising strategy to overcome this problem. It has been reported that Pt–O–Ce and Pt–O–Pt sites have shown strong interactions between O₂ molecules and Pt sites to enhanced nine-

fold catalytic efficiencies for CO oxidation.[22,23] Similarly, Cr–O–Ni reported good H₂O dissociation kinetics and high neutral HER activity due to the enhanced interaction between H₂O molecules and Cr–O–Ni sites.[24] Unfortunately, these systems are easily affected by oxidation of substrates, and no research succeeded in implementing M1–O–M2 sites for alkaline HER.

In this work, we design and demonstrate an alkaline HER Ru/MoO₂ composite with Ru–O–Mo sites, which has chemical stability and strong interaction with H₂O. Theoretical calculations performed with first-principle simulations predict that the engineering of Ru–O–Mo sites enhances H₂O adsorption.[25-29] Such enhancement is driven by the charge transfer from Ru sites to the O sites, brought by higher d-orbital of the surrounding Mo sites, which reduce the H₂O dissociation barrier. Motivated by these theoretical results, we prepare Ru/MoO₂ with Ru–O–Mo sites by a hydrothermal process and pyrolysis treatment. The obtained catalyst shows an overpotentials as low as 16 mV at the current density of 10 mA cm⁻², with a Tafel slope of 32 mV dec⁻¹ in 1 M KOH solution and long-term HER stability over 40 hours.

2. Results and discussion

Figure 1 and S1-2 shows the theoretical results on Ru/MoO₂ with Ru–O–Mo sites by density-functional theory (DFT) calculations. Calculated H₂O adsorption energies show that the Mo sites of Ru–O–Mo have stronger H₂O adsorption ability (2.06 eV)

than Ru (0.35 eV) and MoO₂ (1.30 eV) (**Figure 1a and S3**). Next, we consider the effect of hydrogen binding energy (HBE) on water adsorption/dissociation. As shown in **Figure S4**, the HBE on Ru sites (−0.41 eV) of Ru-O-Mo is stronger than that on Mo sites (0.25 eV) of Ru–O–Mo, indicating that the Ru sites can adsorb hydrogen to further promote the H₂O dissociation process. **Figure 1b** exhibits the charge density difference at the Ru–O–Mo sites. The 1.81 electrons are transferred from Ru to MoO₂ through the Ru–O–Mo sites, weakening the Mo–O bonds in MoO₂, enhancing the interaction of O in H₂O molecules with the Mo sites.[26, 30] This process shorten the distance between the adsorbed H₂O molecule and Ru–O–Mo sites of 2.19 Å, whose value is lower than pure MoO₂ (2.22 Å). These calculations demonstrate that Ru–O–Mo sites enhance the adsorption of H₂O molecules.

Figure 1c reports the energy barriers of H₂O dissociation and H₂ desorption on Ru–O–Mo sites. The energy barrier of H₂O dissociation on Ru–O–Mo of 0.58 eV is significantly lower than that of Ru catalyst (0.81 eV), indicating that Ru–O–Mo sites achieve a better H₂O adsorption and dissociation kinetics than pure Ru theoretically. The reduction of 0.23 eV in the H₂O activation barrier, implying a massive reduction in the energy consumption. For H₂ desorption process, the Gibbs free energy of adsorbed *H (ΔG_{H*}) on the Ru–O–Mo sites (−0.27 eV) is much lower than that of Ru (−0.42 eV), demonstrating the easier desorption process on Ru–O–Mo sites.

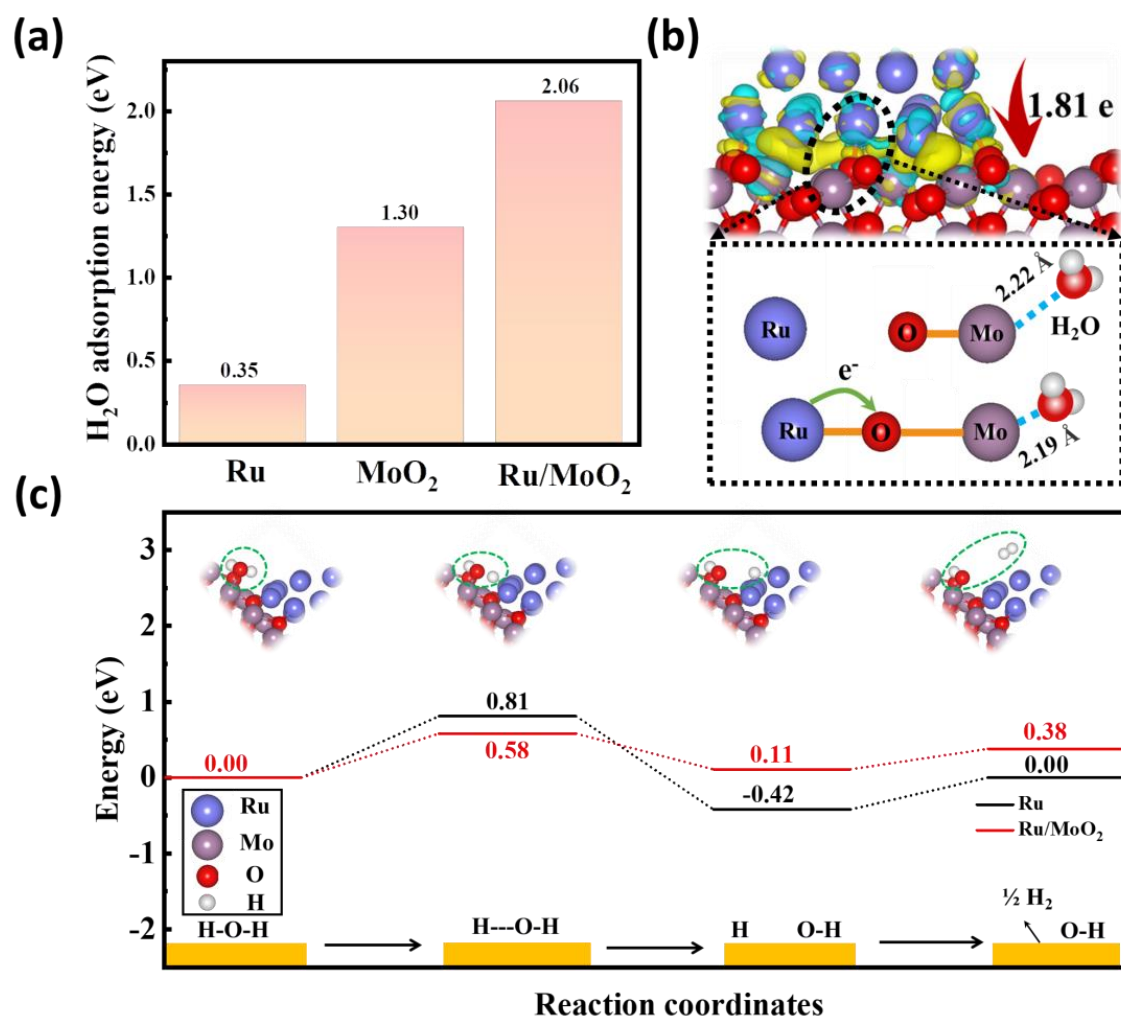


Figure 1. The design principle and DFT calculations of catalysts. (a) The calculated H₂O adsorption energy of Ru, MoO₂, and Ru/MoO₂. (b) The charge density difference and Bader charge transfer at the interface of Ru/MoO₂, and the schematic diagram of charge transfer affecting H₂O adsorption on interface Ru–O–Mo sites. The yellow and blue regions represent electron accumulation and depletion, respectively. (c) The calculated free-energy diagrams of H₂O reduction to H₂ on the surface Ru and Ru/MoO₂ catalysts.

We experimentally prepare Ru/MoO₂ catalyst with paired Ru–O–Mo sites through a facile hydrothermal reaction with a pyrolysis process on a graphite carbon substrate

(**Figure 2a**). Details on the manufacturing process are in the Supporting Information.

Figure S5 reports XRD pattern of obtained Ru/MoO₂ catalyst, showing the presence of MoO₂ (JCPDS 76-1807), and no obvious Ru XRD peaks due to the low Ru content.[18,31] Raman spectra confirm Mo–O bonds with sharp peaks at 479, 816, and 1000 cm⁻¹ [32,33], and a Ru–O bond peak at 646 cm⁻¹ (**Figure S6**).[34] According to the TG-DTA curves (**Figure S7**), each component's resulting content percentages in the catalyst are 21.26 wt% of Ru, 44.0 wt% of MoO₂, and 34.74 wt% of carbon.

We study the morphology of the obtained catalyst by transmission electron microscopy (TEM) (**Figure 2b** and **S8-10**). The small black spots are the Ru/MoO₂ catalyst, which is composed of Ru and MoO₂ nanoparticles with sizes ~2 nm and ~6 nm, respectively. A high-angle annular dark-field (HAADF) STEM image shows a clear interface of Ru–O–Mo sites. **Figure 2c** reports the corresponding lattice fringes, with interplanar spaces of 0.214 nm and 0.244 nm, representing the (002) plane of Ru and the (200) plane of MoO₂, respectively. **Figure 2d** presents energy-dispersive X-ray spectroscopy (EDS) mappings, which show uniform distribution of Ru, Mo, and O elements.

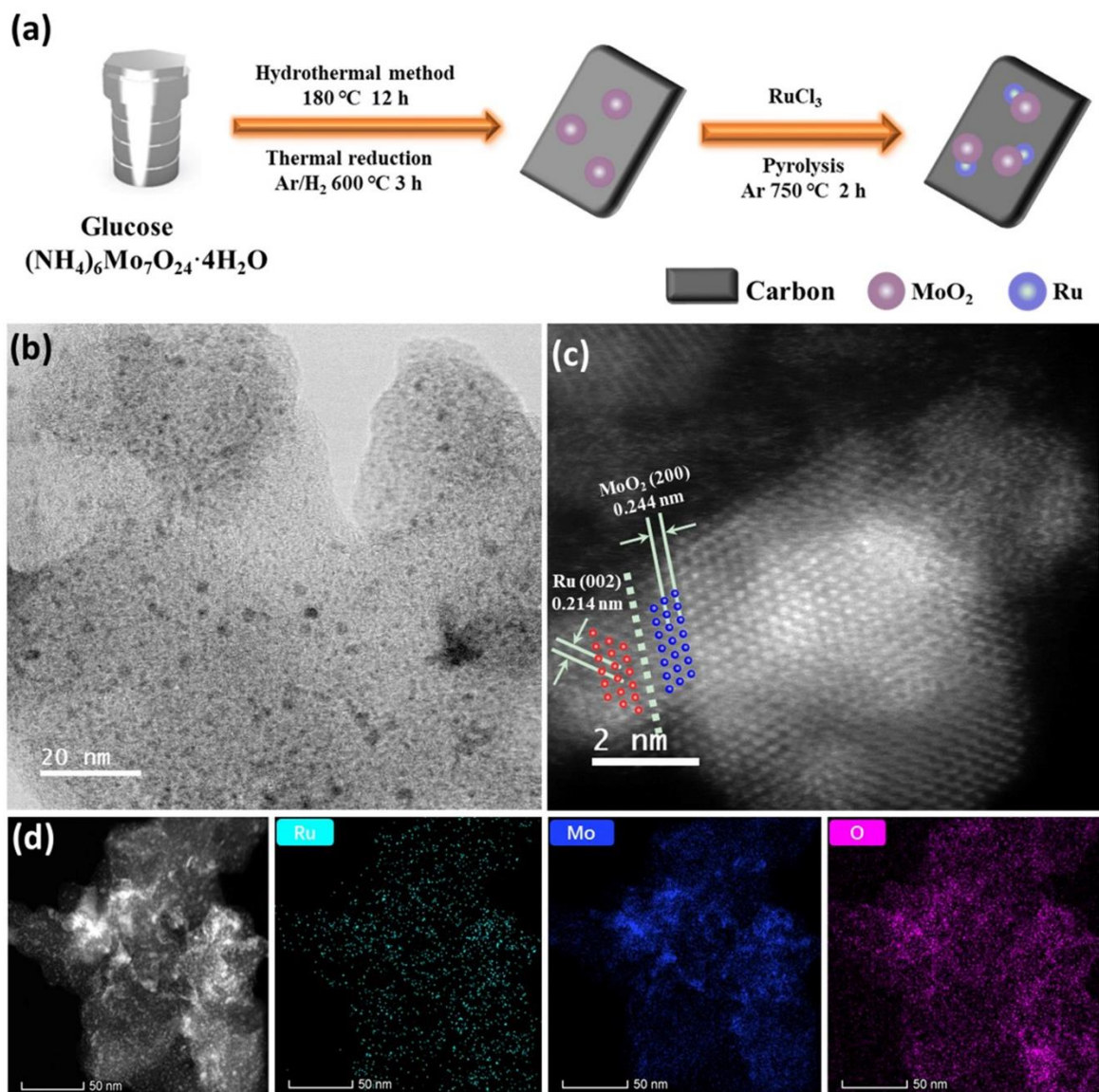


Figure 2. Preparation process and structure characterizations of the catalyst. (a) The schematic diagram of the preparation process of the Ru/MoO₂ catalyst. Typical TEM image (b), HAADF-STEM (c), and EDS mapping images (d) of the Ru/MoO₂ catalyst.

We further investigate the material structure of the catalyst by synchrotron X-ray absorption spectra.[35-37] The extended X-ray absorption fine structure (EXAFS) spectra and their wavelet transform analyses (**Figure 3a-b, S11, and Table S1**) showed

that the obtained Ru/MoO₂ catalyst has clear Ru–O (1.5 Å) and Ru–Ru (2.4 Å) bonds.[38] No peak located at 3.2 Å of Ru–O–Ru bonding is observed in the catalyst, proving Ru–O–Mo sites form between Ru and MoO₂ nanoparticles. The positive shifts of Ru peak observed in both X-ray absorption near edge structure (XANES, **Figure 3c**) and X-ray photoelectron spectroscopy (XPS, **Figure 3d**) spectra of Ru/MoO₂ with Ru–O–Mo sites, further confirms the strong charge transfer from Ru to O. These results are consistent with the Bader charge analyses obtained by DFT calculations.

To prove the enhanced H₂O adsorption/dissociation ability on Ru/MoO₂, we carried out Fourier transfer infrared spectrum (FTIR) and H₂O adsorption tests. **Figure 3e** reports FTIR spectra, in which Ru/MoO₂ shows the strongest hydroxyl response signal among those of MoO₂ and Ru, in the range between 2900 cm⁻¹ ~ 3500 cm⁻¹. [39-43] In the H₂O adsorption tests (**Figure 3f and S12**), the higher current density difference between the cases with and without H₂O proves the larger H₂O adsorption/activation ability of Ru/MoO₂ with Ru–O–Mo sites,[44] which after normalization is between ~2 and ~10 times higher than that of MoO₂ and Ru, respectively. These experimental results confirm the DFT theoretical predictions on H₂O adsorption/dissociation energy.

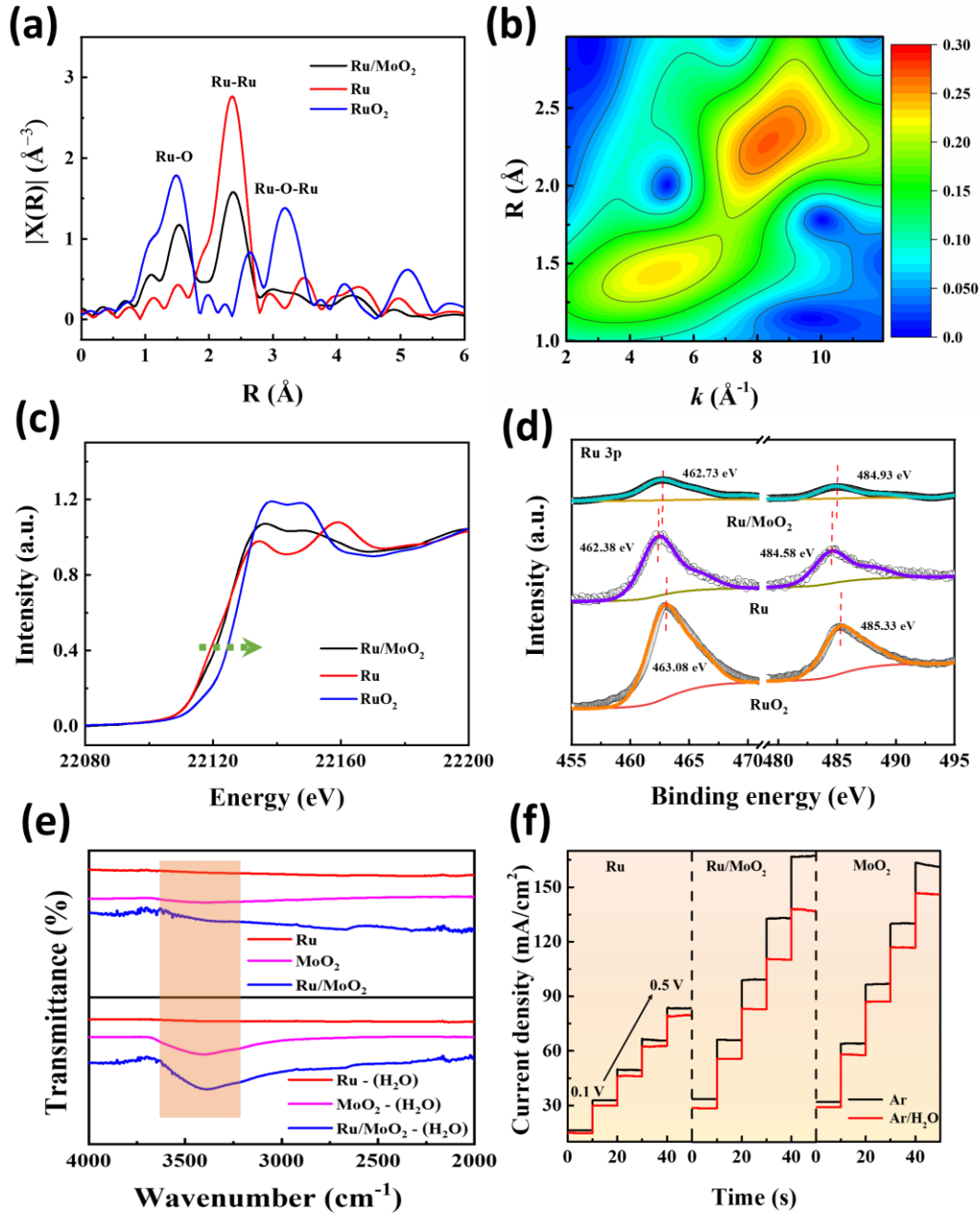


Figure 3. Interface structure, charge transfer, and H₂O adsorption/dissociation ability. (a) Extended X-ray absorption fine structure (EXAFS) spectra of Ru K-edge. (b) The Ru K-edge whole contour plots of wavelet transform (WT) of Ru/MoO₂ catalyst. (c) The enlarged X-ray absorption near edge structure (XANES) spectra of Ru K-edge. (d) High-resolution XPS spectra of Ru 3p of Ru, RuO₂,

and Ru/MoO₂. (e) The FTIR spectra of Ru, MoO₂, and Ru/MoO₂. (f) The H₂O adsorption sensor tests of Ru, MoO₂, and Ru/MoO₂.

We then assess the catalysts' electrocatalytic HER activities in the alkaline solution (1 M KOH) with a standard three-electrode system. As shown in **Figure 4a**, the linear sweep voltammetry (LSV) curves show that the Ru/MoO₂ with Ru–O–Mo sites has largely improved overpotential of 16 mV at 10 mA cm⁻¹, which is more than one order of magnitude lower than the one of MoO₂ (254 mV), and few times smaller than the ones of Ru (59 mV), and Pt (31 mV). The corresponding Tafel slope is 32 mV dec⁻¹, which shows a similar improvement over the 174, 64, and 39 mV dec⁻¹ possessed by Ru, MoO₂, and Pt, respectively (**Figure 4b**). The lower Tafel slope indicates faster HER kinetics of Ru/MoO₂ catalyst. The alkaline HER undergoes two important steps, one is H₂O adsorption/dissociation on the catalyst's surface (Volmer step: H₂O + * + e⁻ → H* + OH⁻), the other is hydrogen (H*) desorption (Tafel/Heyrovsky step: 2H* → H₂/H₂O + H* + e⁻ → H₂ + OH⁻).[12,45] Tafel slope is an important parameter to reflect the rate-determining step of HER. The 174 mV dec⁻¹ indicates the H₂O adsorption/dissociation (Volmer step) is the rate-determining step of Ru. The Tafel slope of 32 mV dec⁻¹ indicates an excellent H₂O adsorption/dissociation ability of Ru/MoO₂, which the rate-determining step transfers from H₂O adsorption/dissociation (Volmer step) to hydrogen (H*) desorption (Tafel/Heyrovsky step). Electrochemical impedance spectroscopy (EIS) is also use to investigate the electrode kinetics in HER.

The Nyquist plots of Ru/MoO₂ and other samples are shown in **Figure S13** and corresponding fitting element parameters are shown in **Table S2**. The R_{ct} of Ru/MoO₂ (24.59 Ω) is lower than Ru (35.53 Ω) and MoO₂ (39.81 Ω). Lower charge transfer resistance corresponds to a faster reaction rate of HER, indicating that Ru/MoO₂ is more active than other samples.

In addition to these benefits, Ru/MoO₂ with Ru–O–Mo sites show good durability in alkaline solutions. In the measurements performed over 5000 cycles, we observed only a small potential drop of 3 mV decayed at 10 mA cm⁻² (**Figure 4c**). Voltage-time curves (**Figure 4c, inset**) show that Ru/MoO₂ catalyst's potential is stable at 100 mA cm⁻² over 40 h. The SEM and XRD characterizations further verify that the morphology and structure of Ru/MoO₂ are well preserved after durability test. (**Figure S14 and S15**) **Figure 4d** and **Table S3**, reporting Tafel slopes and overpotentials at 10 mA cm⁻² with different Ru-based and Pt-based catalysts, demonstrate that the alkaline HER performance of the obtained Ru–O–Mo catalyst is superior to other reported catalysts.

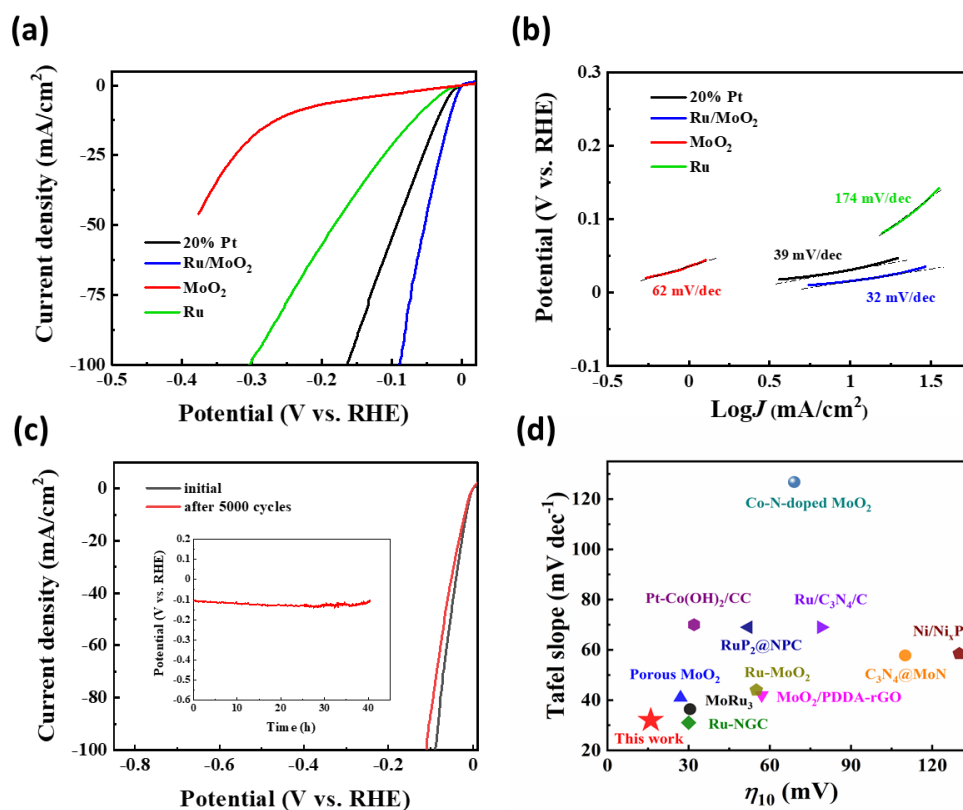


Figure 4. The electrocatalytic HER tests in 1 M KOH solution. (a) Linear scanning voltage (LSV) curves of commercial 20% Pt, Ru, MoO₂, and Ru/MoO₂ in 1 M KOH solution. (b) The corresponding Tafel plots are recorded in (a). (c) Linear scanning voltage curves of Ru/MoO₂ before and after 5000 cycles in 1 M KOH solution. The inset represents the voltage-time curve of Ru/MoO₂ at 100 mA/cm^2 for 40 h. (d) The comparisons of Tafel slopes and overpotentials at 10 mA/cm^2 with different Ru-based and Pt-based catalysts.

3. Conclusions

We designed and implemented an efficient catalyst for HER composed of Ru/MoO₂ with Ru–O–Mo sites. First-principle calculations showed that Ru–O–Mo sites have higher adsorption/dissociation for H₂O than conventional Ru catalysts. We then

prepared Ru/MoO₂ with Ru-O-Mo sites, verifying the existence of Ru–O–Mo with HAADF-STEM images and EXAFS spectra. XANES and XPS experimentally proved the substantial interface charge transfer between Ru and MoO₂, while FTIR and H₂O adsorption tests demonstrated the enhanced H₂O adsorption ability of Ru–O–Mo sites. In a series of electrochemistry measurements, the catalyst implemented with this approach showed an overpotential of 16 mV (at 10 mA cm⁻²), with stability over 40 hours in alkaline HER. This work can help in the design and implementation of highly-efficient alkaline HER catalysts for large scale, sustainable and economical hydrogen production from water splitting.

Acknowledgments

We thank the Natural Science Foundation of China (Grant No. 21872174 and U1932148), International Science and Technology Cooperation Program (Grant No. 2017YFE0127800 and 2018YFE0203402), Hunan Provincial Science and Technology Program (2017XK2026), Hunan Provincial Natural Science Foundation of China (2020JJ2041 and 2020JJ5691), Shenzhen Science and Technology Innovation Project (Grant No. JCYJ20180307151313532), The Hunan Provincial Science and Technology Plan Project (Grant No. 2017TP1001), The Fundamental Research Funds for the Central Universities of Central South University, and MOST 109-2113-M-213-002.

References

- [1] N. Mahmood, Y. Yao, J. W. Zhang, L. Pan, X. Zhang, J. J. Zou, *Adv. Sci.* **2018**, *5*, 1700464.

- [2] Y. Zheng, Y. Jiao, A. Vasileff, S. Z. Qiao, *Angew. Chem. Int. Ed.* **2018**, *57*, 7568.
- [3] Q. Gao, W. Zhang, Z. Shi, L. Yang, Y. Tang, *Adv. Mater.* **2019**, *31*, 1802880.
- [4] J. O. Abe, A. P. I. Popoola, E. Ajenifuja, O. M. Popoola, *Int. J. Hydrogen Energy* **2019**, *44*, 15072.
- [5] C. Hu, L. Zhang, J. Gong, *Energy Environ. Sci.* **2019**, *12*, 2620.
- [6] X. Du, J. Huang, J. Zhang, Y. Yan, C. Wu, Y. Hu, C. Yan, T. Lei, W. Chen, C. Fan, J. Xiong, *Angew. Chem. Int. Ed.* **2019**, *58*, 4484.
- [7] N. Cheng, S. Stambula, D. Wang, M. N. Banis, J. Liu, A. Riese, B. Xiao, R. Li, T. K. Sham, L. M. Liu, G. A. Botton, X. Sun, *Nat. Commun.* **2016**, *7*, 13638.
- [8] R. Subbaraman, D. Tripkovic, D. Strmcnik, K. C. Chang, M. Uchimura, A. P. Paulikas, V. Stamenkovic, N. M. Markovic, *Science* **2011**, *334*, 1256.
- [9] W. Li, Y. Liu, M. Wu, X. Feng, S. A. T. Redfern, Y. Shang, X. Yong, T. Feng, K. Wu, Z. Liu, B. Li, Z. Chen, J. S. Tse, S. Lu, B. Yang, *Adv. Mater.* **2018**, *30*, 1800676.
- [10] F. Li, G. F. Han, H. J. Noh, I. Ahmad, I. Y. Jeon, J. B. Baek, *Adv. Mater.* **2018**, *30*, 1803676.
- [11] Z. Zhang, P. Li, Q. Feng, B. Wei, C. Deng, J. Fan, H. Li, H. Wang, *ACS Appl. Mater. Interfaces* **2018**, *10*, 32171.
- [12] T. Zhang, M.-Y. Wu, D.-Y. Yan, J. Mao, H. Liu, W.-B. Hu, X.-W. Du, T. Ling, S.-Z. Qiao, *Nano Energy* **2018**, *43*, 103.
- [13] H. Jin, X. Liu, Y. Jiao, A. Vasileff, Y. Zheng, S.-Z. Qiao, *Nano Energy* **2018**, *53*, 690.
- [14] Z. Zhang, P. Li, Q. Wang, Q. Feng, Y. Tao, J. Xu, C. Jiang, X. Lu, J. Fan, M. Gu, H. Li, H. Wang, *J. Mater. Chem. A* **2019**, *7*, 2780.
- [15] B. Lu, L. Guo, F. Wu, Y. Peng, J. E. Lu, T. J. Smart, N. Wang, Y. Z. Finrock, D. Morris, P. Zhang, N. Li, P. Gao, Y. Ping, S. Chen, *Nat. Commun.* **2019**, *10*, 631.
- [16] J. Mahmood, F. Li, S. M. Jung, M. S. Okyay, I. Ahmad, S. J. Kim, N. Park, H. Y. Jeong, J. B. Baek, *Nat. Nanotech.* **2017**, *12*, 441.
- [17] T. Qiu, Z. Liang, W. Guo, S. Gao, C. Qu, H. Tabassum, H. Zhang, B. Zhu, R. Zou, Y. Shao-Horn, *Nano Energy* **2019**, *58*, 1.
- [18] J. Ding, Q. Shao, Y. Feng, X. Huang, *Nano Energy* **2018**, *47*, 1.
- [19] X. Qin, L. Zhang, G.-L. Xu, S. Zhu, Q. Wang, M. Gu, X. Zhang, C. Sun, P. B. Balbuena, K. Amine, M. Shao, *ACS Catal.* **2019**, *9*, 9614.
- [20] C. Clay, S. Haq, A. Hodgson, *Chem. Phys. Lett.* **2004**, *388*, 89.
- [21] S. Maier, I. Stass, J. I. Cerda, M. Salmeron, *Phys. Rev. Lett.* **2014**, *112*, 126101.
- [22] X. I. Pereira-Hernandez, A. DeLaRiva, V. Muravev, D. Kunwar, H. Xiong, B. Sudduth, M. Engelhard, L. Kovarik, E. J. M. Hensen, Y. Wang, A. K. Datye, *Nat Commun* **2019**, *10*, 1358.
- [23] H. Wang, J. X. Liu, L. F. Allard, S. Lee, J. Liu, H. Li, J. Wang, J. Wang, S. H. Oh, W. Li, M. Flytzani-Stephanopoulos, M. Shen, B. R. Goldsmith, M. Yang, *Nat Commun* **2019**, *10*, 3808.

- [24] C. T. Dinh, A. Jain, F. P. G. de Arquer, P. De Luna, J. Li, N. Wang, X. Zheng, J. Cai, B. Z. Gregory, O. Voznyy, B. Zhang, M. Liu, D. Sinton, E. J. Crumlin, E. H. Sargent, *Nat. Energy* **2018**, 4, 107.
- [25] S. Deng, X. Liu, X. Guo, T. Zhao, Y. Lu, J. Cheng, K. Chen, T. Shen, Y. Zhu, D. Wang, *J. Energy Chem.* **2021**, 54, 202.
- [26] Z. W. Seh, J. Kibsgaard, C. F. Dickens, I. Chorkendorff, J. K. Norskov, T. F. Jaramillo, *Science* **2017**, 355, 146.
- [27] K. Liu, J. Fu, L. Zhu, X. Zhang, H. Li, H. Liu, J. Hu, M. Liu, *Nanoscale* **2020**, 12, 4903.
- [28] J. Fu, K. Liu, K. Jiang, H. Li, P. An, W. Li, N. Zhang, H. Li, X. Xu, H. Zhou, D. Tang, X. Wang, X. Qiu, M. Liu, *Adv. Sci.* **2019**, 6, 1900796.
- [29] P. An, L. Wei, H. Li, B. Yang, K. Liu, J. Fu, H. Li, H. Liu, J. Hu, Y.-R. Lu, H. Pan, T.-S. Chan, N. Zhang, M. Liu, *J. Mater. Chem. A* **2020**, 8, 15936.
- [30] L. Fu, Y. Li, N. Yao, F. Yang, G. Cheng, W. Luo, *ACS Catalysis* **2020**, 10, 7322.
- [31] C. Cai, S. Han, Q. Wang, M. Gu, *ACS Nano* **2019**, 13, 8865.
- [32] R. Prabhu B, K. Bramhaiah, K. K. Singh, N. S. John, *Nanoscale Adv.* **2019**, 1, 2426.
- [33] L. O. Alemn-Vzquez, E. Torres-Garca, J. R. Villagmez-Ibarra, J. L. Cano-Domnguez, *Catal. Lett.* **2005**, 100, 219.
- [34] Z. J. Han, S. Pineda, A. T. Murdock, D. H. Seo, K. Ostrikov, A. Bendavid, *J. Mater. Chem. A* **2017**, 5, 17293.
- [35] C. Cai, M. Wang, S. Han, Q. Wang, Q. Zhang, Y. Zhu, X. Yang, D. Wu, X. Zu, G. E. Sterbinsky, Z. Feng, M. Gu, *ACS Catal.* **2020**, 11, 123.
- [36] V. Ramalingam, P. Varadhan, H.-C. Fu, H. Kim, D. Zhang, S. Chen, L. Song, D. Ma, Y. Wang, H. N. Alshareef, J. H. He, *Adv. Mater.* **2019**, 31, 1903841.
- [37] X. Wang, Y. Zhu, A. Vasileff, Y. Jiao, S. Chen, L. Song, B. Zheng, Y. Zheng, S.-Z. Qiao, *ACS Energy Letters* **2018**, 3, 1198.
- [38] Q. He, D. Tian, H. Jiang, D. Cao, S. Wei, D. Liu, P. Song, Y. Lin, L. Song, *Adv. Mater.* **2020**, 32, 1906972.
- [39] K. Jiang, L. Zhu, Z. Wang, K. Liu, H. Li, J. Hu, H. Pan, J. Fu, N. Zhang, X. Qiu, M. Liu, *Appl. Surf. Sci.* **2020**, 508, 145173.
- [40] G. Busca, The surface acidity of solid oxides and its characterization by IR spectroscopic methods. An attempt at systematization, *Phys. Chem. Chem. Phys.* **1999**, 1, 723.
- [41] A. Celino, O. Goncalves, F. Jacquemin, S. Freour, *Carbohydr. Polym.* **2014**, 101, 163.
- [42] H. A. Al-Hosney, V. H. Grassian, *Phys. Chem. Chem. Phys.* **2005**, 7, 1266.
- [43] Yunfeng Lu, Ling Han, C. Jeffrey Brinker, Thomas M. Niemczyk, G. P. Lopez, *Sensors and Actuators B* **1996**, 35-36, 517.
- [44] S. Cao, Y. Chen, H. Wang, J. Chen, X. Shi, H. Li, P. Cheng, X. Liu, M. Liu, L. Piao, *Joule* **2018**, 2, 549.
- [45] D. Kim, J. Park, J. Lee, Z. Zhang, K. Yong, *ChemSusChem* **2018**, 11, 3618.

